Journal of Applied Polymer Science

Morphology, Rheology, Crystallization Behavior, and Mechanical Properties of Poly(lactic acid)/Poly(butylene succinate)/Dicumyl Peroxide Reactive Blends

Deyun Ji, Zhengying Liu, Xiaorong Lan, Feng Wu, Banghu Xie, Mingbo Yang
State Key Laboratory of Polymer Materials Engineering, College of Polymer Science and Engineering, Sichuan University, Chengdu, 610065, Sichuan, People's Republic of China
Correspondence to: Z. Liu (E-mail: liuzhying@scu.edu.com)

ABSTRACT: The reactive blends were prepared by the blending of poly(lactic acid) (PLA) with poly(butylene succinate) (PBS) in the presence of dicumyl peroxide (DCP) as a radical initiator in the melt state. The gel fractions, morphologies, crystallization behaviors, and rheological and mechanical properties of the reactive blends were investigated. Some crosslinked/branched structures were formed according to the rheological measurement and gel fraction results, and the crosslinked/branched structures played the role of nucleation site for the reactive blends. The PLA–PBS copolymers of the reactive blends acted as a compatibilizer for the PLA and PBS phases and, hence, improved the compatibility between the two components. Moreover, it was found that the reactive blends showed the most excellent mechanical properties as the DCP contents were 0.2 and 0.3 phr. © 2013 Wiley Periodicals, Inc. J. Appl. Polym. Sci. **2014**, *131*, 39580.

KEYWORDS: biopolymers & renewable polymers; biodegradable; blends

Received 10 March 2013; accepted 22 May 2013
DOI: 10.1002/app.39580

INTRODUCTION

More recently, the development and use of biodegradable polymers from renewable resource has drawn much attention. Among those materials, poly(lactic acid) (PLA) is supposed to be one of the most promising aliphatic polyesters because of its good mechanical strength and excellent transparency.[1–3] With the environmental pollution and limited resources taken into consideration, more and more researchers have been making efforts to apply PLA to replace some petrol materials in the industry field because of its biodegradability, biocompatibility, and so on.[4,5] However, many drawbacks, including a poor impact strength, small elongation at break, and low heat distortion temperature,[6] restrict the application of PLA in many fields, such as food packaging and industrial engineering. One of the effective approaches used to overcome these drawbacks is the blending of PLA with other flexible polymers. In recent years, blends of PLA with many degradable and nondegradable polymers, such as polyethylene,[7,8] polycaprolactone,[9–13] poly (butylene–adipate-*co*-terephthalate) (PBAT),[14,15] and poly (butylene succinate) (PBS),[16–18] have been widely studied. However, most of the blending products showed poor mechanical performance because of the low miscibility between the components of the blends. Reactive processing is considered to be an effective method for improving the miscibility of PLA blends. Zhang et al.[19] and Kumar et al.[20] used glycidyl methacrylate (GMA) as a processing agent for PLA/PBAT blends, and the results revealed that the PLA–PBAT copolymer formed after the use of GMA was able to enhance the interfacial adhesion between the two components. Furthermore, with 2 or 5 wt % GMA, the tensile toughness of the PLA/PBAT blend was greatly increased without a severe loss in the tensile strength. Lysine triisocyanate is also a useful reactive processing agent for increasing the compatibility of PLA/PBS blends, as reported by Harada et al.,[21] and the results revealed that the impact strength of PLA/PBS (90/10 w/w) increased remarkably in the presence of lysine triisocyanate at 0.5 wt %. Twice-functionalized organoclay (TFC) was incorporated into the poly-L-lacitc acid (PLLA)/PBS blend as an *in situ* reactive compatibilizer in the research of Chen et al.[22] As the TFC content increased, the clay layers were dispersed in both the PBS and PLLA phases, and the domain size of the dispersed PBS phase became significantly smaller. In addition, the addition of TFC to the PLLA/PBS blend not only improved the tensile modulus but also improved the elongation at break. Sometimes, dicumyl peroxide (DCP) has been introduced into PLA/PBAT, PLA/polycaprolactone, and PLA/PBS blends as an initiator to form crosslinked and/or branched structures by heterogeneous and/or homogeneous radical coupling reactions.[23–27] The copolymers formed between

Table I. Compositions of the Reactive Blends and Codes for All of the Specimens

Sample	PLA (g)	PBS (g)	DCP (g)
PLA	100	0	0
P-S20D0	80	20	0
P-S20D1	80	20	0.1
P-S20D2	80	20	0.2
P-S20D3	80	20	0.3
P-S20D4	80	20	0.4
P-S20D5	80	20	0.5

the two phases by heterogeneous reactions could improve the compatibility of the polymer blends and, therefore, enhance the mechanical properties of the reactive blends.

In the past, research on the reactive blending of PLA has mostly focused on the mechanical properties; however, the crystallization behavior of the PLA reactive blends has scarcely been investigated. To the best of our knowledge, the study of the crystallization behavior is vital for polymer because of the fact that many properties of the final products are related to the crystallization morphology formed during processing.

In this study, PLA/PBS/DCP reactive blends were prepared with DCP as an initiator in the melt state. Then, the crystallization behavior of the PLA/PBS/DCP reactive blends was investigated. In addition, the mechanical properties, miscibility, phase morphology, and rheological properties of the reactive blends were also investigated.

EXPERIMENTAL

Materials

PLA was supplied by Zhejiang Hisun Biomaterials Co., Ltd., with a weight-average molecular weight (M_w) of 100,000 g/mol. The PBS (HX-B601, M_w = 120,000 g/mol) used in this study was obtained from Anqing He Xing Chemical Corp., Ltd. DCP with a half-life of 1 min at 175°C was purchased from Kelong Chemical Reagent Co. (Chengdu, China) and was used as a radical initiator. Chloroform was used without further purification. PLA and PBS pellets were dried in a vacuum oven at 60°C for 24 h before melt blending.

Sample Preparation

The blends were prepared in an internal mixer (XSS-300 torque rheometer; Kechuang Mechanical Equipment, Shanghai, China) at 180°C and a screw speed of 50 rpm. The compounding procedures included two steps. First, PLA/PBS (80/20 wt/wt) raw particles were introduced into the internal mixer, which achieved the setting temperature for 1 min. Second, different amounts of DCP were added to the mixer, and the blending procedure was continued for 9 min after the addition of DCP. The blend formulations and code are shown in Table I. Pure PLA was treated with the same process to compare with the blends with equivalent thermomechanical histories. The torque change was recorded during the whole mixing process. The obtained materials were cut into small pieces and dried at 60°C overnight in a vacuum oven before further processing and measurement. Sheets with a thickness of 0.6 mm for mechanical testing were prepared with a hot press at 180°C and a pressure of 10 MPa for 3 min and then with a cold press at the same pressure for 2 min.

The samples for rheological testing were prepared by compression molding at 180°C for about 5 min in the form of disks 25 mm in diameter and with a thickness of 1.5 mm. To prevent water absorption, the blends obtained were stored in a vacuum oven at 60°C for at least 24 h before usage.

Measurements and Characterization

The gel content of the reactive blend was estimated through measurement of the amount of the insoluble part in chloroform for 48 h at room temperature. The gel fraction was calculated as follows:[28,29]

$$\text{Gel fraction}\,(\%) = 100(W_d/W_i)$$

where W_i is the initial weight of the dried sample after reactive blending and W_d is the weight of the dried insoluble part of sample after extraction.

The morphology of the blends was observed by scanning electron microscopy (SEM; JEOL JSM-5900LV, JEOL Pte., Ltd., Tokyo, Japan) at an acceleration voltage of 5 kV. The blend samples were fractured after immersion in liquid nitrogen for about 30 min. The fracture surfaces were coated with gold to make them electrically conducting.

The crystallization and crystallization kinetics were studied by differential scanning calorimetry (DSC; Q20, TA Instruments, Inc., New Castle, DE). The nonisothermal crystallization behavior of all of the samples was monitored at a cooling rate of 10°C/min after they were heated to 190°C and held at that temperature for 5 min. Also, to investigate the melting behavior, all of the samples were heated to 190°C at a rate of 10°C/min.

In the isothermal crystallization kinetic experiments, the samples were first heated to 190°C and then held at that temperature for 5 min to erase any thermal history. Subsequently, the sample was rapidly cooled to the isothermal crystallization temperature of 110°C. All of the samples were held at the desired isothermal temperature until no changes in the heat flow were observed.

During the isothermal crystallization process, the heat flow (dH/dt) over the crystallization time could be obtained via DSC. The isothermal heat flow curve was integrated to determine the relative crystallinity (X_t) as a function of crystallization time with eq. (1):[30]

$$X_t = {}^{t}\frac{\int_0^t (dH/dt)dt}{\int_0^\infty (dH/dt)dt} \quad (1)$$

where the first integral represents the heat (H) generated at time t, whereas the second integral represents the total heat generated up to the end of the isothermal crystallization process.

Generally, the isothermal crystallization kinetics analysis of these samples is performed with the following Avrami equation:[31,32]

$$X_t = 1 - exp(-kt^n) \quad (2)$$

where k is the crystallization rate constant and n is the Avrami exponent, whose value depends on the geometry of the growing

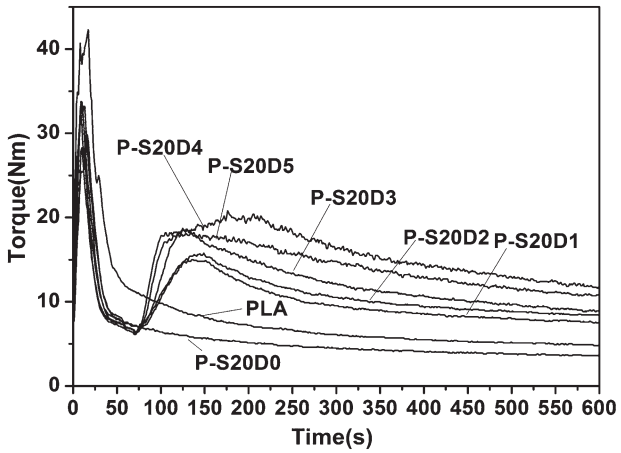

Figure 1. Torque-time trend recorded for the neat PLA and PLA/PBS (80/20 wt %) blends treated with different percentages of DCP.

crystallites. For the sake of dealing conveniently with the operation, eq. (2) is usually rewritten as a double logarithmic form as follows:

$$\log[-\ln(1-X_t)] = \log k + n\log t \quad (3)$$

Accordingly, n and k can be obtained from the slope and intercept, respectively. Meanwhile, the crystallization half-time ($t_{1/2}$) is the time at which the extent of crystallization is 50%; this is defined as $t_{1/2} = (\ln 2/k)^{1/n}$.

The shear rheological properties of each blend and neat PLA were carried out on a stress-controlled rheometer (AR2000EX, TA Instruments) with a 25-mm parallel-plate geometry. All of the measurements were performed at 180°C and a frequency range of 0.01–10 rad/s under a nitrogen atmosphere to prevent degradation. All of the samples were dried in a vacuum oven before the test.

Testing of the mechanical properties of pure PLA and the PLA/PBS/DCP reactive blends were performed with a universal testing machine (AGS-J, Japan) at room temperature and with a crosshead speed of 5 mm/min. Dog-bone-shaped specimens with a gauge length of 20 mm and a width of 4 mm were cut from sheets 0.6 mm thick obtained by compression molding. The values of the tensile strength and elongation at break were obtained on the basis of the average tensile results of at least five tensile specimens.

RESULTS AND DISCUSSION

Torque Values of PLA/PBS with or Without DCP During Processing

Figure 1 shows the torque value of the pure PLA and the PLA/PBS blends with and without DCP during the melting or reactive blending. The torque value decreased sharply at the beginning of the introduction of pure PLA or PLA/PBS blends without DCP into the internal mixer, and then it became smooth and steady with increasing processing time. Notably, the torque value increased rapidly when DCP was added to the PLA/PBS blends compared with the PLA/PBS blends without DCP. As we know, the torque value depends on the molecular weight and chain structure of the polymer under a constant temperature and shear stress;[33] it could be speculated that some crosslinked/branched structures were formed during reactive blending because of the addition of DCP. That is, some chemical bonds between PLA and PLA, PBS and PBS, and PLA and PBS would formed by heterogeneous and/or homogeneous radical coupling reactions by the addition of DCP as a reaction initiator.[26] In addition, it seems that the higher the DCP content was, the higher the torque value was obtained. However, the torque value of P-S20D5 was less than that of P-S20D4.

The probable reactions of the reactive blends that led to crosslinked/branched structures are proposed in Scheme 1.[22,26,34,35] First, the organic peroxide decomposed to free radicals under heating. Second, the free radical extracted the secondary hydrogen from the α-carbon atom of PLA or PBS to yield free radicals on the main chain of PLA or PBS. Compared with PLA, the molecular structure of PBS with many secondary hydrogen atoms facilitated easy abstraction of hydrogen atoms by peroxide. Furthermore, β scission occurred to yield a primary radical with regard to the PBS component. On the other hand, PLA had tertiary carbon atoms of which the generated radical was stabilized even under melt conditions so that the β scission of PLA did not occur by the addition of DCP.[26] Finally, the crosslinked/branched structures of PLA or PBS via homogeneous radical coupling reactions and PLA–PBS copolymers via radical coupling between the primary/secondary radicals of PBS and the radicals of PLA were formed. As a result, these crosslinked/branched structures played a great role in changing the viscoelasticity of the reactive blends; this was proven by the torque–time trend record and the following rheology characterizations.

Gel Fraction of the Reactive Blends

The gel fraction of the PLA/PBS/DCP reactive blends with different contents of DCP is shown in Figure 2. The gel fraction increased with increasing content of DCP. Notably, the increase in the gel content slowed when the DCP percentage was more than 0.3 phr.

Morphology of PLA/PBS Blends with Different Contents of DCP

The SEM results for the phase morphology characterization of the blends are depicted in Figure 3. The phase separation of the PLA/PBS blend without DCP (P-S20D0) are shown clearly in Figure 3(a). Spherical droplets of PBS were found in the PLA continuous phase. Noticeably, the size of the PBS dispersed phase

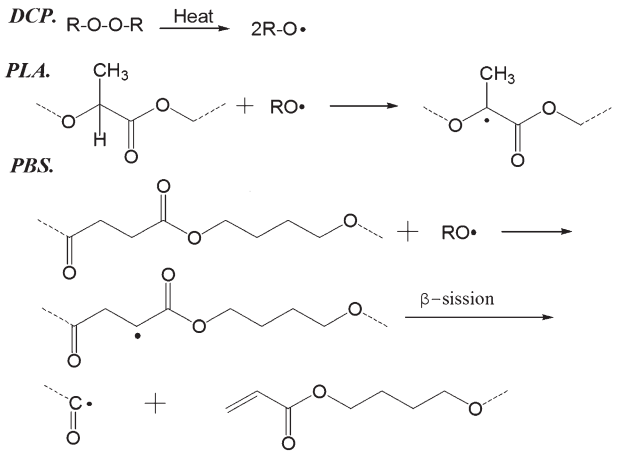

Scheme 1. Predicted reaction mechanisms for the PLA/PBS blends with DCP addition.

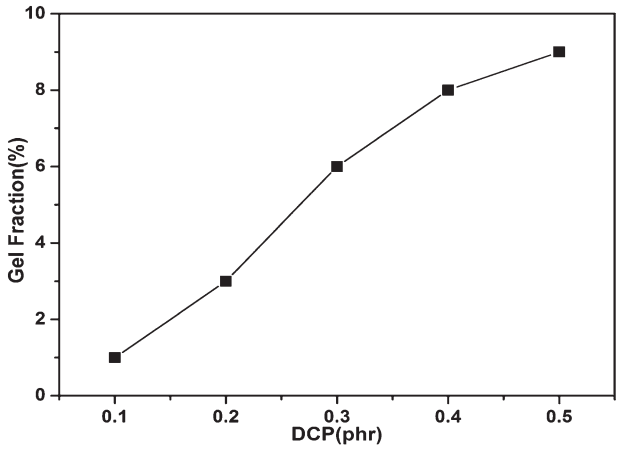

Figure 2. Gel fraction of the reactive blends with different amounts of DCP.

became smaller, and the distance between PLA and PBS phase decreased and even disappeared in the reactive blends, as shown in Figure 3(b–f); this indicated that the compatibility of PLA and PBS was improved even when a little DCP was added. This result may be explained as follows: the PLA–PBS copolymer formed during blending according to the Fourier transform infrared results, acting as a good compatibilizer, decreased the interfacial tension and increased the interfacial adhesion between PLA and PBS. What is more, as shown in Figure 3(d–f), some small granules dispersed in the matrix, which referred to some crosslinked structures formed after the addition of DCP.

Rheological Properties of the PLA/PBS/DCP Reactive Blends

The responses of the frequency to the storage modulus (G'), loss angle tangent value (tan δ), and complex viscosity at 180°C for the neat PLA and PLA/PBS/DCP reactive blends are illustrated in Figure 4. According to Figure 4(a,b), with respect to G' of the PLA blended with PBS alone that is, P-S20D0, it was similar to that of the research of Bhatia et al.[37] It was also clearly observed that G' of the reactive blend melts increased with increasing DCP dosage, especially at low frequencies. In addition, the tan δ values of PLA and P-S20D0 were higher than that of the reactive blends, and the greater the amount of DCP was added, the higher the tan δ was obtained. These were due to the fact that some crosslinked/branched structures formed after the addition of DCP, enhanced the melt elasticity,[38] and made the chain easer to entangle in the matrix.[39] In other words, the entanglement density and melt elasticity of the PLA/PBS/DCP reactive blends were higher than those of the PLA and PLA/PBS blend without DCP that is, P-S20D0.

As shown in Figure 4(c), the pure PLA and PLA/PBS blend without DCP (P-S20D0) displayed a Newtonian liquid behavior at low frequencies. Moreover, P-S20D0 also showed a higher complex viscosity because of the high molecular weight of the PBS component. For the reactive blends, a higher complex viscosity and distinct shear thinning behavior could be seen during the investigated frequency range. The pronounced shear thinning behavior of the reactive blends was attributed to the generated crosslinked/branched structures, which enhanced the chain entanglement in the PLA/PBS matrix[40] and was in combination with the G' and tan δ results.

Nonisothermal Crystallization and Melting Behavior for PLA/PBS Blends with or Without DCP

The effect of the crosslinked/branched structures on the crystallization behavior of the PLA/PBS/DCP reactive blends were investigated through the nonisothermal and isothermal

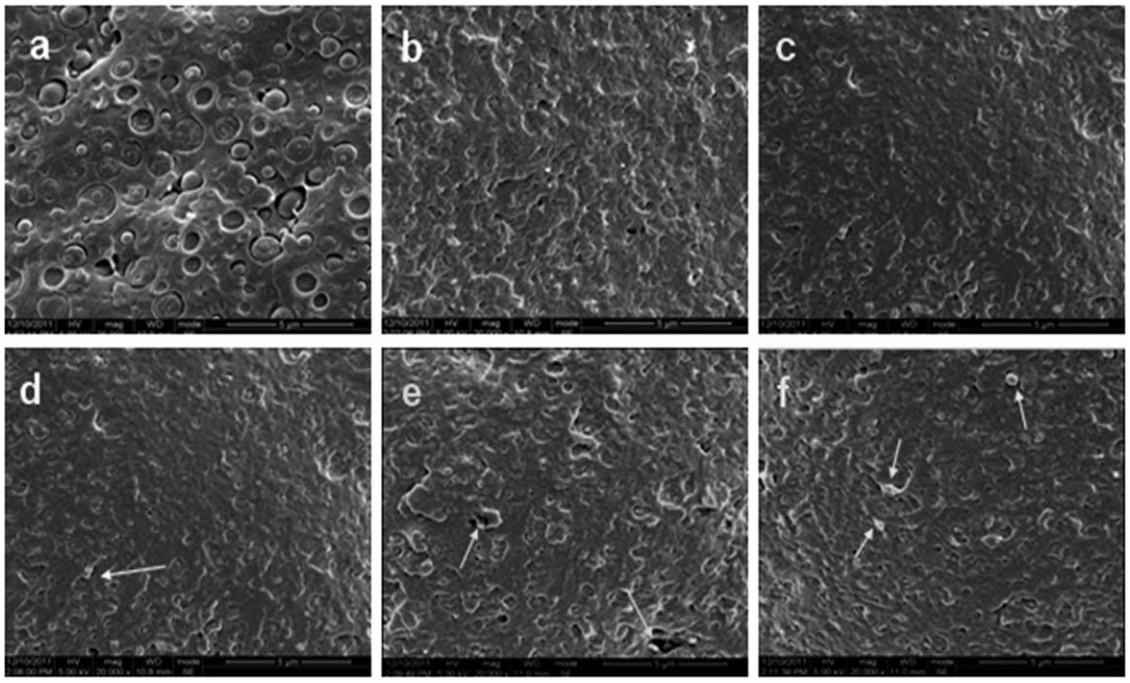

Figure 3. SEM images of the PLA/PBS/DCP blends: (a) P-S20D0, (b) P-S20D1, (c) P-S20D2, (d) P-S20D3, (e) P-S20D4, and (f) P-S20D5.

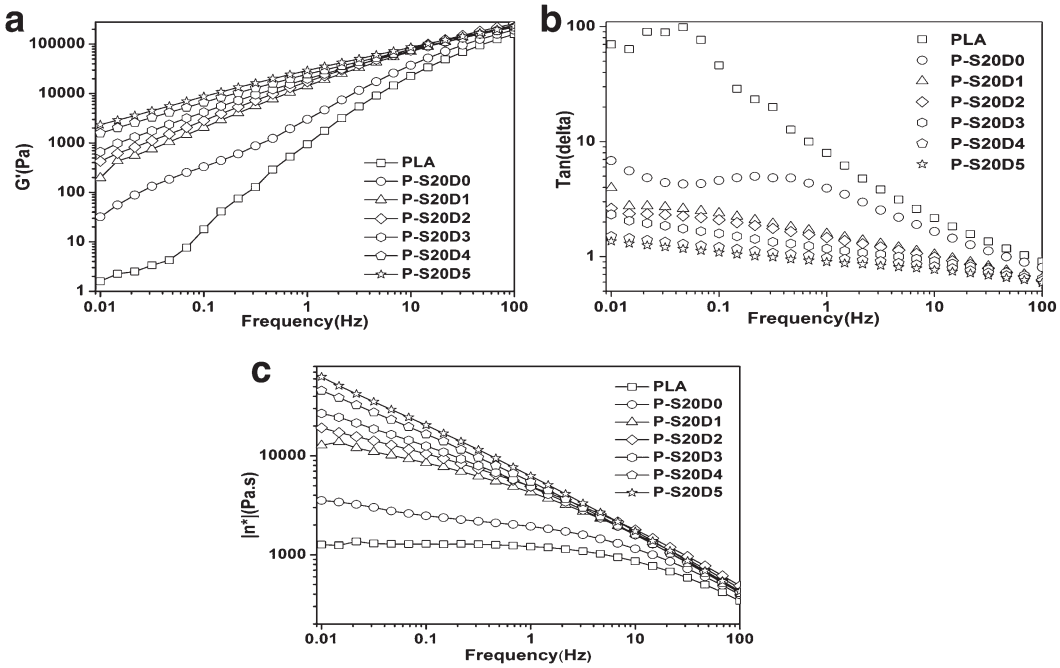

Figure 4. (a) G', (b) tan δ, and (c) complex viscosity ($|\eta^*|$) of the pure PLA and PLA/PBS/DCP reactive blends at 180°C.

crystallization research. Figure 5(a) displays the cooling process for all of the samples. We clearly observed that pure PLA could not undergo crystallization at a cooling rate of 10°C/min, whereas PBS crystallized at the same cooling rate.

To our great surprise, different crystallization behaviors were observed as the DCP was added to the PLA/PBS/DCP reactive blends. As is shown in Figure 5(a), when the content of DCP was less than 0.3 phr, the crystallization of the PBS component occurred. According to the studies of Kim et al.[41] and Nofar et al.,[42] crosslinked/branched structures formed during reactive blending may act as nucleation agents in the reactive blend matrix. We speculated that most of the crosslinked/branched structures were formed by PBS (this was in accordance with the reaction scheme for the reactive blends) when the amount of the DCP was low, and these crosslinked/branched structures acted as nucleating sites, which improved the crystallization of the PBS component. Meanwhile, small numbers of the crosslinked/branched structures were formed for the PLA component as the lower DCP contents were added. That is, fewer nucleation sites were generated for PLA in the same situation with regard to PBS. When the content of DCP was above 0.3 phr, the PLA phase underwent crystallization, and the crystallization ability of the PLA phase was clearly improved with increasing DCP; we concluded from this that more nucleating sites were generated in the PLA phase when more DCP was added. In addition, as the DCP content increased, the crystallization peak of the PBS component was gradually weakened and even disappeared. It could also be seen that the crystallization temperature of the PLA phase increased with DCP content but decreased with the PBS component; this implied that the PLA crystallization hindered the PBS crystallization.

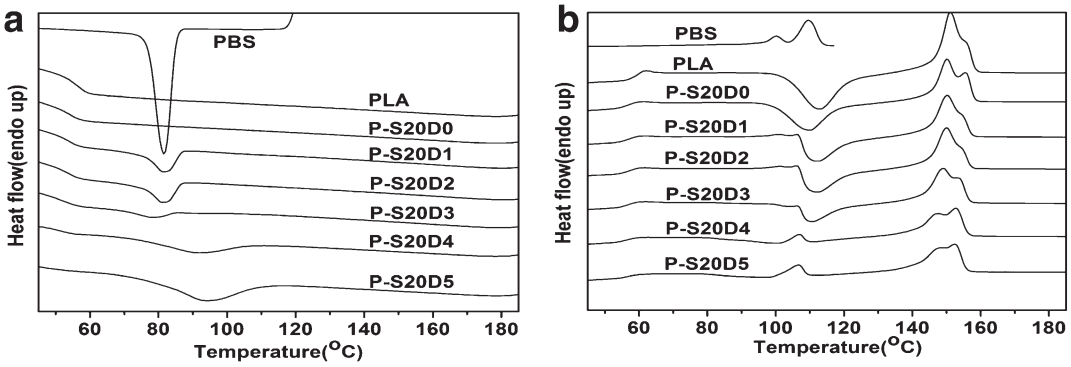

Figure 5. DSC curves for all of the samples (a) cooling at a rate of 10°C/min and (b) heating at a rate of 10°C/min.

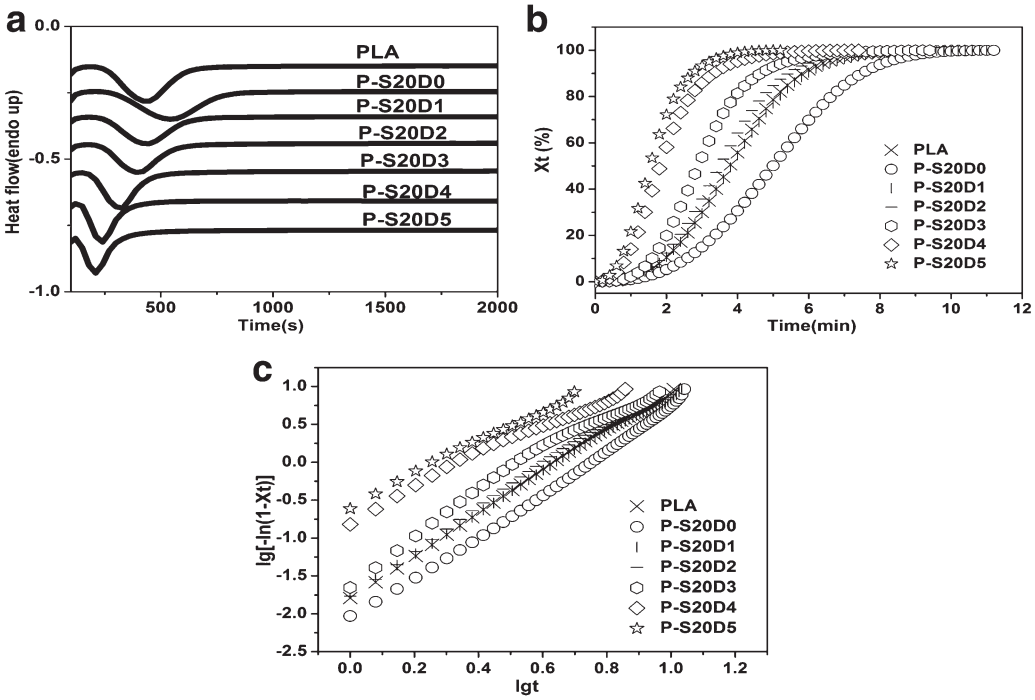

Figure 6. (a) DSC curves, (b) development of X_t with time, and (c) Avrami plots of $\log[-\ln(1 - X_t)]$ versus $\log t$ of the isothermal crystallization of the PLA/PBS/DCP reactive blends at 110°C.

The melting behavior for all of the samples is shown in Figure 5(b). The glass-transition temperature of the reactive blends was nearly equal to that of the pure PLA, whereas the cold crystallization peak of PLA around 110°C was gradually weakened, especially when more than 0.3 phr of DCP was incorporated. This indicated that the addition of DCP enhanced the crystallization ability of the PLA phase during cooling from the melt state. The cold crystallization peak of PLA was partly overlapped with the melt peak of PBS, which was around 105°C.[43] The cold crystallization peak of PLA decreased continuously, and the melt peak of the PBS component became more obvious with increasing DCP content, and it became more obvious when the DCP content was more than 0.3 phr. A melt peak with a shoulder around 155°C appeared for pure PLA because the recrystals melted at higher temperature. However, it was obvious that the shoulder melting peak for reactive blends became more remarkable with increasing DCP, and the reasons could be summarized as follows. For the PLA/PBS/DCP reactive blends, the crosslinked/branched structures formed during blending acted as nucleation sites on the one hand but reduced the chains mobility on the other hand. Therefore, imperfect and small size crystals were likely to be generated for the reactive blends. Consequently, the recrystallization behavior was more likely to occur for the reactive blends compared with pure PLA; as a result, the shoulder melting peak was much sharper than that of pure PLA.

Isothermal Crystallization of the PLA/PBS Blends with or Without DCP

Isothermal crystallization was studied to research the effect of the crosslinked/branched structures on the crystallization kinetics of the PLA/PBS/DCP reactive blends. Figure 6(a) presents the isothermal thermograms of the pure PLA and PLA/PBS/DCP reactive blends at 110°C. We found that the total time for accomplishing the crystallization of P-S20D0 was longer than that of the pure PLA; this implied that the crystallization rate for PLA was hindered when it was blended with PBS alone. However, the addition of DCP shortened the total isothermal crystallization time for the reactive blends; this indicated an increase in the crystallization rate. In addition, the total time for completing the crystallization of the reactive blends decreased with increasing content of DCP; the crosslinked/branched structures might have formed during the reactive blending might and acted as nucleation agents in the reactive blend matrix. Hence, the crystallization rate of the PLA component was accelerated during isothermal crystallization.

Table II. Avrami Kinetic Parameters from the Avrami Equation and Values of X_c for the PLA/PBS/DCP Reactive Blends

Sample	n	k (min^{-1})	$t_{1/2}$ (min)	X_c (%)[a]
PLA	2.81	0.0152	3.89	30.41
P-S20D0	2.79	0.0080	4.96	29.94
P-S20D1	2.76	0.0171	3.82	29.01
P-S20D2	2.96	0.0166	3.53	27.76
P-S20D3	2.99	0.0232	3.11	26.57
P-S20D4	2.44	0.1556	1.84	25.98
P-S20D5	2.24	0.2577	1.56	25.76

[a] X_c (%) = 100(ΔH_m/93), where ΔH_m is enthalpy of melting, 93 was taken to be the enthalpy of melting for pure PLA crystal.[42]

Table III. Mechanical Properties of the PLA/PBS/DCP Reactive Blends

Sample	Tensile strength (MPa)	Elongation at break (%)
PLA	89	20
P-S20D0	55	49
P-S20D1	68	134
P-S20D2	73	195
P-S20D3	80	205
P-S20D4	77	151
P-S20D5	72	92

The plots of X_t as a function of time are shown in Figure 6(b). X_t of the blends was greater than that of pure PLA at a certain crystallization time except for P-S20D0. In addition, the time for accomplishing the crystallization of the samples gradually reduced with increasing content of DCP. These results illustrate that the crystallization rate of the reactive blends was enhanced in the attendance of DCP compared with that of pure PLA.

The plots of $\log[-\ln(1 - X_t)]$ versus $\log t$ for isothermal crystallization of the PLA/PBS/DCP reactive blends are shown in Figure 6(c). The n, k, and $t_{1/2}$ values for the pure PLA and PLA/PBS/DCP reactive blends calculated from these plots are summarized in Table II. The value of k was related to the nucleation rate and growth processes. From the data shown in Table II, it was obvious that the k values of the reactive blends was higher than that of pure PLA; this meant that the crystallization rate was increased for the reactive blends. $t_{1/2}$ is usually used to characterize the crystallization rate. For all of the reactive blends, the $t_{1/2}$ value decreased with increasing DCP content; this illustrated that the crystallization rate of the reactive blends matrix was improved compared with pure PLA.

Furthermore, for the pure PLA and reactive blends with contents of DCP less than 0.4 phr, the n value approached 3, whereas it got closer to 2 for P-20D4 and P-S20D5. In addition, the degree of crystallization (X_c; %) decreased for the reactive blends with respect to the pure PLA, and the greater the content of DCP was, the lower the X_c was obtained. According to these results, we speculated reasonably that although the crosslinked/branched structures enhanced the crystal nucleation, the chain mobility was decreased. In a word, the crosslinked/branched structures had two different effects on the crystallization of the reactive blends. One was the positive effect on the nucleation; the other was the negative effect on the crystal growth.

Mechanical Properties of the PLA/PBS Blends with or Without DCP

Table III summarizes the tensile properties of the PLA/PBS/DCP reactive blends. For pure PLA, it had a high tensile strength and a low elongation at break. The incorporation of PBS partly improved the ductility of PLA (P-S20D0). With regard to the PLA/PBS/DCP reactive blends, the tensile strength increased with increasing DCP when the DCP content was less than 0.3 phr; it decreased with the continuing increase in the dosage of DCP. The elongation at break of the reactive blends displayed the same trend with respect to the DCP content. Furthermore, P-S20D2 and P-S20D3, that is, when the DCP content was 0.2 and 0.3 phr, respectively, in the reactive blend matrix, the specimens showed the most excellent mechanical properties. This was attributed to the fact that the compatibility of P-S20D2 and P-S20D3 was significantly improved because of the few formed PLA–PBS copolymers. However, when more DCP was added, even more crosslinked structures were obtained; this might have done harm to the mechanical properties of the reactive blends.[26]

CONCLUSIONS

In this study, the crystallization, mechanical, morphological, and rheological properties of the PLA/PBS blends in the presence of DCP were investigated. From the results of torque, gel fraction, and rheological property testing, we deduced that some crosslinked/branched structures were formed in the reactive blend matrix. In particular, the introduction of DCP resulted in the improvement of compatibility between PLA and PBS according to the SEM analysis because PLA–PBS copolymers were formed after the addition of DCP. Moreover, the isothermal crystallization of PLA was enhanced with regard to the reactive blends because the crosslinked/branched structures could act as nucleating agents for PLA or PBS. Furthermore, there was an interesting find in that the crystallization behavior of the PLA and PBS components presented interchange phenomenon with regard to the reactive blends in the nonisothermal crystallization process; this was attributed to fact that the PBS generated crosslinked/branched structures more easily than PLA, and the PLA crystallization hindered the crystallization of PBS. In addition, the mechanical properties were also improved when an appropriate content of DCP was added. On the basis of the tensile test results, the reactive blends, especially P-S20D2 and P-S20D3, showed a considerably higher elongation at break, whereas there was a small decrease in the tensile strength compared with pure PLA.

ACKNOWLEDGMENTS

The authors acknowledge the financial support of this work by the National Natural Science Foundation of China (contract grant number 51033003).

REFERENCES

1. Inkinen, S.; Hakkarainen, M.; Albertsson, C. A.; Sodergard, A. *Biomacromolecules* **2011**, *12*, 523.
2. Stoclet, G.; Seguela, R.; Lefebvre, J. M. *Polymer* **2011**, *53*, 1417.
3. Liu, H. Z.; Chen, F.; Liu, B.; Estep, G.; Zhang, J. W. *Macromolecules* **2010**, *43*, 6058.
4. Tsuji, H.; Fukui, I. *Polymer* **2003**, *44*, 2891.
5. Lee, J. B.; Lee, Y. K.; Choi, G. D.; Na, W. S.; Park, T. S.; Kim, W. N. *Polym. Degrad. Stab.* **2011**, *96*, 553.
6. Hashima, K.; Nishitsuji, S.; Inoue, T. *Polymer* **2010**, *51*, 3934.
7. Anderson, K. S.; Hillmyer, M. A. *Polymer* **2004**, *45*, 8809.
8. Anderson, K. S.; Lim, S. H.; Hillmyer, M. A. *J. Appl. Polym. Sci.* **2003**, *89*, 3757.

9. Zhang, G. B.; Zhang, J. M.; Wang, S. G.; Shen, D. Y. *J. Polym. Sci.* **2003**, *41*, 23.
10. Chen, H. P.; Pyda, M.; Cebe, P. *Thermochim. Acta* **2009**, *492*, 61.
11. Erba, R. D.; Groeninckx, G.; Maglio, G.; Malinconico, M.; Migliozzi, A. *Polymer* **2001**, *42*, 7831.
12. Takayama, T.; Todo, M. *J. Mater. Sci.* **2006**, *41*, 4989.
13. Rezgui, F.; Swistek, M.; Hiver, J. M.; Sell, C. G.; Sadoun, T. *Polymer* **2005**, *46*, 7370.
14. Yeh, J. T.; Tsou, C. H.; Huang, C. Y.; Chen, K. N.; Wu, C. S.; Chai, W. L. *J. Appl. Polym. Sci.* **2010**, *116*, 680.
15. Coltelli, M. B.; Toncelli, C.; Ciardelli, F.; Bronco, S. *Polym. Degrad. Stab.* **2011**, *96*, 982.
16. Park, S. B.; Hwang, S. Y.; Moon, C. W.; Im, S. S. *Macromol. Res.* **2010**, *18*, 463.
17. Shibata, M.; Inoue, Y.; Miyoshi, M. *Polymer* **2006**, *47*, 3557.
18. Shibata, M.; Teramoto, N.; Inoue, Y. *Polymer* **2007**, *48*, 2768.
19. Zhang, N. W.; Wang, Q. F.; Ren, J.; Wang, L. *J. Mater. Sci.* **2009**, *44*, 250.
20. Kumar, M.; Mohanty, S.; Nayak, S. K.; Parvaiz, M. R. *Bioresour. Technol.* **2010**, *101*, 8406.
21. Harada, M.; Ohya, T.; Iida, K.; Hayashi, H.; Hirano, K.; Fukuda, H. *J. Appl. Polym. Sci.* **2007**, *106*, 1813.
22. Chen, G. X.; Kim, H. S.; Kim, E. S.; Yoon, J. S. *Polymer* **2005**, *46*, 11829.
23. Semba, T.; Kitagawa, K.; Kotaki, M.; Hamada, H. *J. Appl. Polym. Sci.* **2008**, *108*, 256.
24. Kanzawa, T.; Tokumitsu, K. *J. Appl. Polym. Sci.* **2011**, *121*, 2908.
25. Semba, T.; Kitagawa, K.; Ishiaku, U. S.; Kotaki, M.; Hamada, H. *J. Appl. Polym. Sci.* **2007**, *103*, 1066.
26. Semba, T.; Kitagawa, K.; Ishiaku, U. S.; Hamada, H. *J. Appl. Polym. Sci.* **2006**, *101*, 1816.
27. Wang, R. Y.; Wang, S. F.; Zhang, Y.; Wan, C. Y.; Ma, P. M. *Polym. Eng. Sci.* **2009**, *49*, 26.
28. Quynh, T. M.; Mitomo, H.; Nagasawa, N.; Wada, Y.; Yoshii, F.; Jamada, M. *Eur. Polym. J.* **2007**, *43*, 1779.
29. Yang, S. L.; Wu, Z. H.; Yang, W.; Yang, M. B. *Polym. Test.* **2008**, *27*, 957.
30. Krikorian, V.; Pochan, D. *J. Macromolecules* **2004**, *37*, 6480.
31. Ke, T. Y.; Sun, X. Z. *J. Appl. Polym. Sci.* **2003**, *89*, 1203.
32. Ojijo, V.; Malwela, T.; Ray, S. S.; Sadiku, R. *Polymer* **2012**, *53*, 505.
33. Liu, J. Y.; Lou, L. J.; Yu, W.; Liao, R.; Li, R.; Zhou, C. X. *Polymer* **2010**, *51*, 5186.
34. Carlson, D.; Dubois, P.; Nie, L.; Narayan, R. *Polym. Eng. Sci.* **1998**, *38*, 311.
35. Coltelli, M. B.; Bronco, S.; Chinea, C. *Polym. Degrad. Stab.* **2010**, *95*, 332.
36. Sirisinha, K.; Somboon, W. *J. Appl. Polym. Sci.* **2012**, *124*, 4986.
37. Bhatia, A.; Gupta, R. K.; Bhattacharya, S. N.; Choi, H. *J. Korea-Aust. Rheol. J.* **2007**, *19*, 125.
38. Borsig, E.; Van, D. M.; Gotsis, A. D.; Picchioni, F. *Eur. Polym. J.* **2008**, *44*, 200.
39. Gu, S. Y.; Zhang, K.; Ren, J.; Zhan, H. *Carbohydr. Polym.* **2008**, *74*, 79.
40. Incarnato, L.; Scarfato, P.; Maio, L. D.; Acierno, D. *Polymer* **2000**, *41*, 6825.
41. Kim, D. J.; Kim, W. S.; Lee, D. H.; Min, K. E.; Park, L. S.; Kang, I. K.; Jeon, I. R.; Seo, K. H. *J. Appl. Polym. Sci.* **2001**, *81*, 1115.
42. Nofar, M.; Zhu, W. L.; Park, C. B.; Randall, J. *Ind. Eng. Chem. Res.* **2011**, *50*, 3798.
43. Lee, S.; Lee, J. W. *Korea-Aust. Rheol. J.* **2005**, *17*, 71.
44. Fisher, E. W.; Sterzel, H. J.; Wegner, G.; Koll, Z. Z. *Polymer* **1973**, *251*, 980.